

Article type : Research Article

Date Received : 29/06/2021

Date Accepted : 12/07/2021

Date published : 01/09/2021



: www.minarjournal.com

<http://dx.doi.org/10.47832/2717-8234.3-3.9>



INFLUENCE OF LASER ENERGY ON CDS NANO PARTIALS PREPARED BY LASER INDUCED PLASMA

Hayim Ch, MAGID¹, Intesar Hato HASHIM ² & Kadhim A. AADIM³

Abstract

In this work ,cadmium sulfide (CdS) thin films deposited on glass substrates using Nd-YAG laser wavelength (1064 nm) laser-induced plasma deposition technique (PLD). The structural, morphology and optical properties of these films have been described as a change in the effect of laser pulse energy ($E = 400, 500, 600$ and 700 mJ). The X-ray diffraction results show that s all samples were polycrystalline hexagonal structure and the crystalline size gchange with increasing of the laser energy. The optical properties results show that the transmittance of all deposited thin films decreases with increasing of laser pulse energy .As a result of the microscopic examination of the surface, it was found that the surface is uniform and the granular size increases with the increase of the laser power.

Keywords: Cadmium Sulfide, Pulsed Laser Deposition, XRD, The Laser Pulse Energy.

¹ Al-Mustansiriyah University, Iraq, halhelfy@yahoo.com

² Al-Mustansiriyah University, Iraq, dr.intesarhatto@yahoo.com, <https://orcid.org/0000-0001-8540-4546>

³ Baghdad University, Iraq, kadhim_adem@scbaghdad.edu.iq, <https://orcid.org/0000-0003-4533-5309>

Introduction

Cadmium sulfide (CdS) material has attracted much attention due to its application in optical-electro devices, such as solar cells and light emitting diodes. Owing to the wide band gap of about 2.4–2.5 eV. CdS polycrystalline thin films are widely used as the window material in hetero junction solar cells. CdS can crystallize in hexagonal (h) wurtzite and cubic (c) zinc blende structures, in which the hexagonal structure is more stable than the cubic structure. Since Sulphur is a volatile element, CdS is prone to generate lattice defect during fabrication procedures. For CdS, interstitial Cd atoms and S vacancies act as donors, and Cd vacancies and interstitial S atoms behave like acceptors. These native defects introduce trapping states into the energy gap, which can significantly influence the optical-electric properties of CdS material [1,2]. CdS is a nonstoichiometric n-type semiconductor with direct band gap energy. In order to allow most of the optically excited electrons to pass through the film, the densities of trapping and recombination centers have to be relatively low. A low resistivity and a high photosensitivity are required for photoconductive-sensor applications. The band gap of CdS is in the range of visible light so the photosensitivity of CdS film in this range very high [3,4]. CdS polycrystalline films have been grown by a variety of film deposition techniques such as thermal evaporation [5], sputtering [6], pulsed laser deposition [7], and chemical bath deposition (CBD) [8]; in each of these methods polycrystalline, uniform and hard films are obtained, and their electrical properties are very sensitive to the method of preparation [9].

In this work CdS thin films were prepared by laser-induced plasma deposition technique (PLD) and study structural properties, electrical properties and atomic force microscopy.

2. Experimental Procedure

Using pulsed laser ablation technique with high purity (99.99 %) cadmium oxide powder factory in FLUK A chemicals limited was used as a source for deposition of CdS films on soda lime glass substrates (2.5x5) cm². The glass substrate was first treated with detergent and washed respectively in running water and alcohol concentration (96 %). Then, the substrates dried with a fine tissue paper and washed in an ultrasonic cleaner with isopropyl alcohol (IPA). The powder mixture was pressed cold at 10-6 Pa films using a hydraulic press, The CdS thin film were prepared by sublimated plasma vapors by generating them with a PLD laser device pulsed, the 1064 nm Nd: YAG laser wavelength was used. The rate of repetition was 10 Hz and the target fluency was set at 60 J / cm² for all samples. At 2.5 cm, the distance from the target to the quartz substratum was preserved. For all experiments the number of shoot 100 has been preserved. The films were deposited at same substrate room temperatures. X-ray diffraction (XRD) investigated the crystal structure of 40 kV and 250 mA films with a reference Cu and a mono-chromometer. Films thickness was change with laser energy at (400mj ,t=173nm),(500mj ,t=162nm).(600mj,t=185nm),(700mj,t=205nm) and (800mj, t=224nm) Weighing method was used to measure film thickness with the full

$$m = 2\pi r^2 \rho \dots (1)$$

Where m is the mass of the substance that has been evaporated, r is the distance between the boat and the substratum, the density of the material being miss. The UV-VIS spectrophotometer was used to test optical properties of the optical transmission spectra of the deposited thin films were calculated as a function of the photon energy in the 300-800 nm wavelength range.

3. Results and Discussion

A. Structural and Morphological Properties.

Figure (1) show the X-ray diffraction patterns of CdS thin film prepared with different laser energies. It can be observed from the figure that all samples showed polycrystalline hexagonal structure matched with the standard card (No. 96-900-8863). Many peaks appeared to conform the lattice planes (100), (002), (101), (102), (110), (103), and (112) at diffraction angles 24.9168°, 26.6001°, 28.2575°, 36.7518°, 43.7699°, 47.9652°, and 51.9793°. There are few variances in the positions of the peaks with rising laser energy due to the difference in lattice uniform strain with

the variation of crystalline size [10]. It is also evident that the peak's intensity increases while the peaks width is decreases with rising laser energy indicates on increasing the crystallinity and growing crystalline size. Increasing the crystalline size with laser energy due to more laser energy enables it to remove larger masses of the target material, as well as the higher energy leads to the merging of the small particles between them [11].

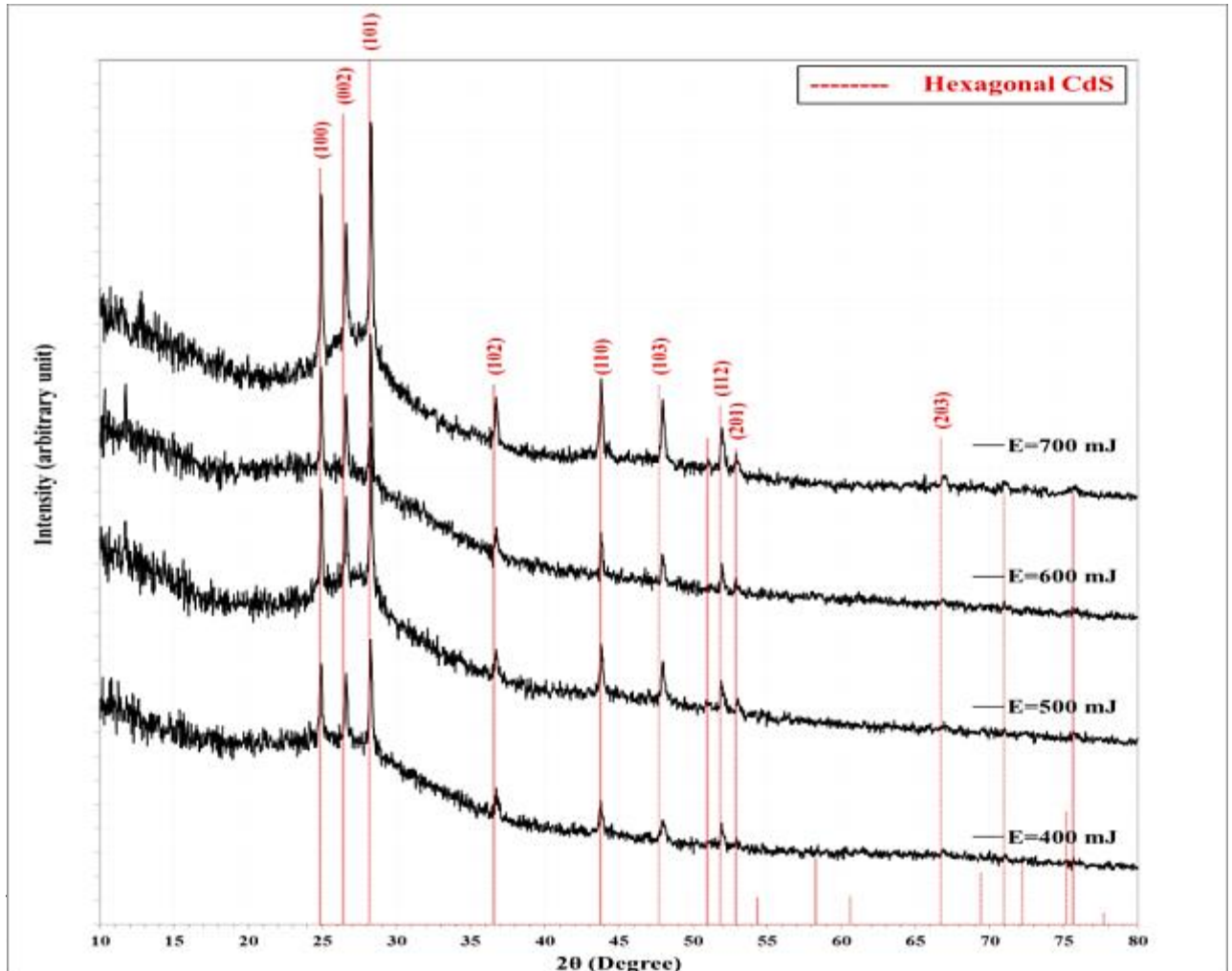


Figure (1): XRD patterns for CdS thin films prepared using different laser energies.

crystalline size (C.S), and corresponding Miller indices. There is a good match between the calculated and standard dhkl values.

Table (1): The variation of XRD parameters for CdS at laser energies different.

E (mJ)	2θ (Deg.)	FWHM (Deg.)	dhkl Exp.(Å)	C.S (nm)	dhkl Std.(Å)	Phase	Hkl
400	24.9168	0.2330	3.5707	34.9	3.5808	Hex.CdS	(100)
	26.6001	0.2072	3.3484	39.4	3.3745	Hex.CdS	(002)
	28.2575	0.2072	3.1557	39.5	3.1632	Hex.CdS	(101)
	36.7518	0.2848	2.4435	29.4	2.4558	Hex.CdS	(102)
	43.7699	0.2849	2.0666	30.1	2.0674	Hex.CdS	(110)
	47.9652	0.3885	1.8951	22.4	1.9049	Hex.CdS	(103)

	51.9793	0.3108	1.7578	28.4	1.7629	Hex.CdS	(112)
500	24.9168	0.2071	3.5707	39.3	3.5808	Hex.CdS	(100)
	26.6260	0.1813	3.3452	45.0	3.3745	Hex.CdS	(002)
	28.2834	0.2072	3.1528	39.5	3.1632	Hex.CdS	(101)
	36.7000	0.2071	2.4468	40.4	2.4558	Hex.CdS	(102)
	43.7958	0.2331	2.0654	36.7	2.0674	Hex.CdS	(110)
	47.9652	0.2849	1.8951	30.5	1.9049	Hex.CdS	(103)
	51.9275	0.3108	1.7595	28.4	1.7629	Hex.CdS	(112)
	53.0411	0.2072	1.7251	42.9	1.7306	Hex.CdS	(201)
600	24.9168	0.1812	3.5707	44.9	3.5808	Hex.CdS	(100)
	26.6001	0.1813	3.3484	45.0	3.3745	Hex.CdS	(002)
	36.7259	0.2589	2.4451	32.3	3.1632	Hex.CdS	(101)
	43.7958	0.2331	2.0654	36.7	2.4558	Hex.CdS	(102)
	47.9134	0.2590	1.8971	33.6	2.0674	Hex.CdS	(110)
	51.9793	0.2590	1.7578	34.1	1.9049	Hex.CdS	(103)
	52.9116	0.1813	1.7290	48.9	1.7629	Hex.CdS	(112)
	700	24.9168	0.1812	3.5707	44.9	3.5808	Hex.CdS
26.6001		0.1813	3.3484	45.0	3.3745	Hex.CdS	(002)
28.2834		0.2331	3.1528	35.1	3.1632	Hex.CdS	(101)
36.7000		0.2330	2.4468	35.9	2.4558	Hex.CdS	(102)
43.7958		0.2590	2.0654	33.1	2.0674	Hex.CdS	(110)
47.9393		0.2331	1.8961	37.3	1.9049	Hex.CdS	(103)
51.9793		0.3108	1.7578	28.4	1.7629	Hex.CdS	(112)
52.9375		0.2849	1.7283	31.1	1.7306	Hex.CdS	(201)
66.9478		0.3625	1.3966	26.3	1.4009	Hex.CdS	(203)

Figure (2) shows the AFM results for CdS surface morphology prepared at different laser energies.

The behavior is same as that shown in the previous samples but with a smaller average size. Increasing the laser pulses energy cause to increase in the average size and the surface roughness as shown.

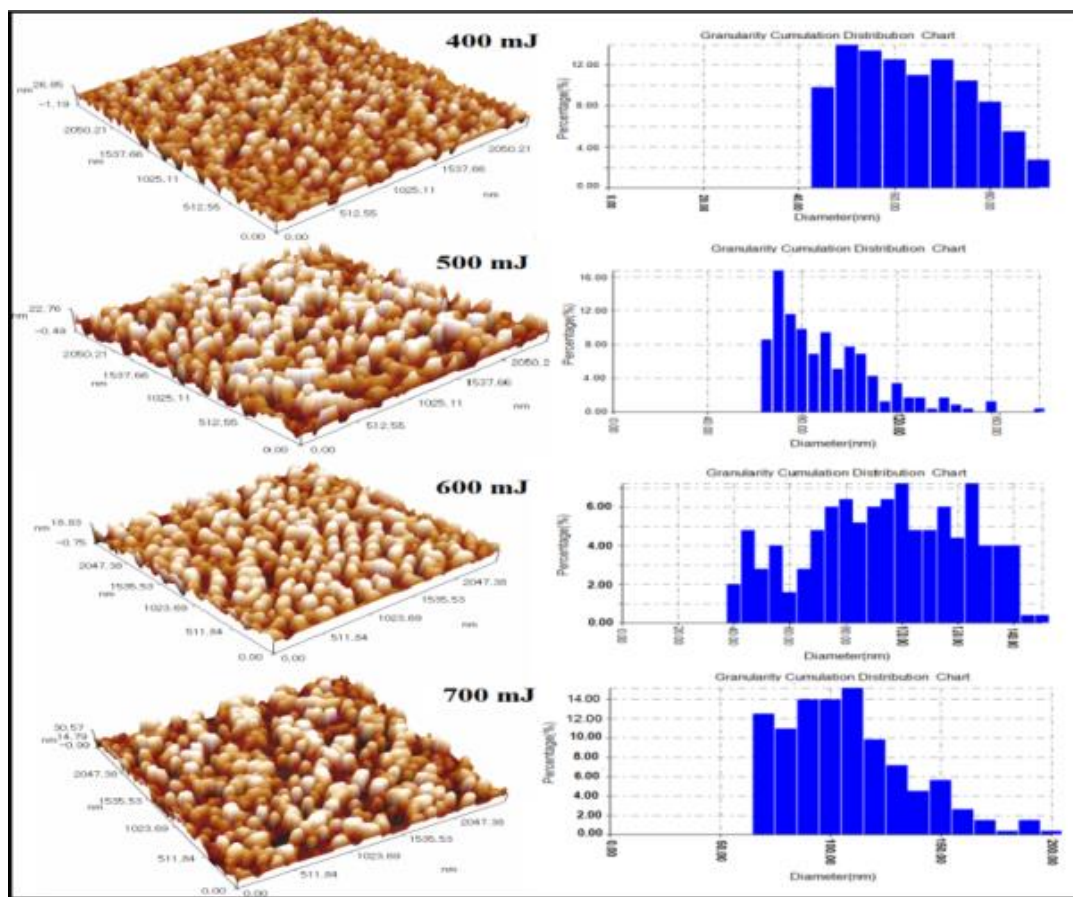


Figure (2): AFM images for CdS thin films surface prepared using different laser energy.

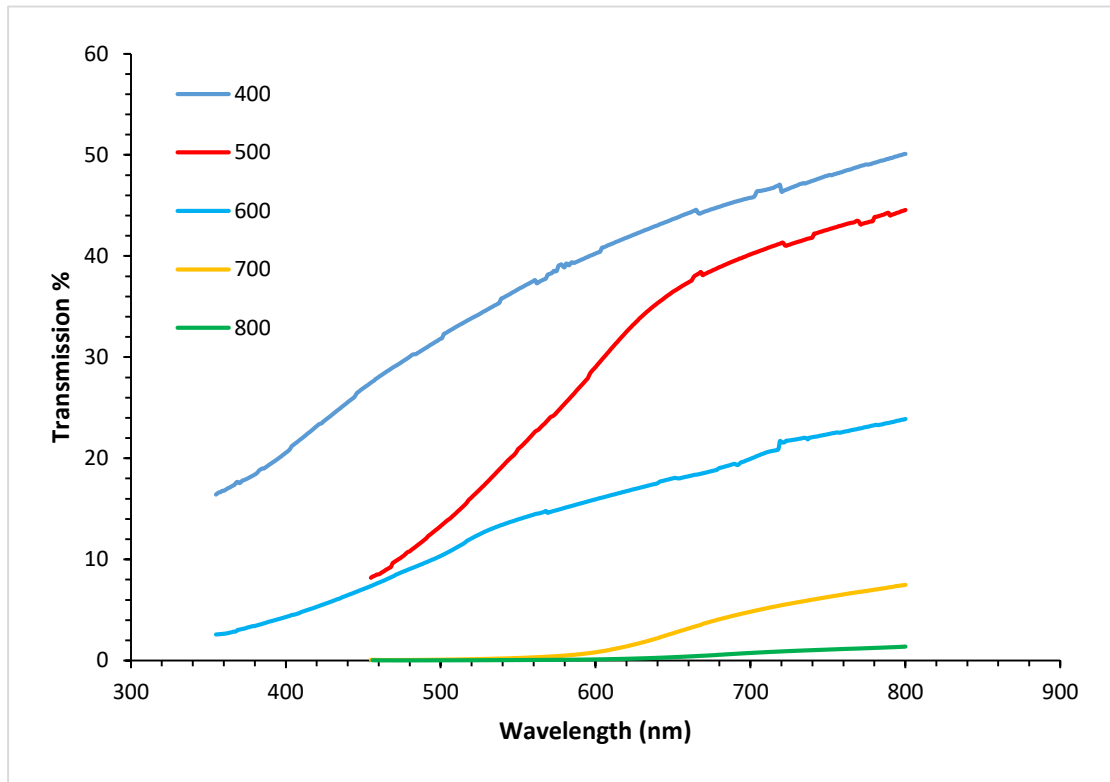
Table (2): AFM parameters (Average Diameter, Average roughness and RMS roughness for CdS thin film prepared using laser energies different

Laser energy (mJ)	Average Diameter (nm)	Average roughness (nm)	RMS roughness (nm)
400	61.34	4.51	5.62
500	87.54	4.42	5.19
600	91.84	6.04	7.05
700	102.35	7.89	9.11

B. Optical Properties

1-transmission

Figure (3) shows the transmission spectrum of CdS thin film prepared at different laser energies. Generally, with increasing laser energy, the transmittance of all deposited thin films decreases. due to an increase in thin-film thickness as a result of the increase in the ablated matter from the target with increasing the laser energy. The transmittance curve shows that all films deposited from plasma vapors have high transparency in the visible and near-infrared regions. The maximum value of optical transmittance is about (45%) that recorded for film with lower energy (400 mJ).



figuer(3): Transmittance spectra as a function of wavelength for CdS films deposited at different laser energies.

2- The Optical Energy Gap

As the energy divide has widened, a fundamental and very important role in determining the applications of the membrane used, for example in detectors and solar cells, must be greater than the energy gap of the base.

The allowed direct The energy difference is calculated by plotting $(\alpha h\nu)^2$. The Tauc equation was used to calculate the photon energy as a function of photon energy. After that, the optical energy gap (E_g) is calculated by extrapolating the portion at $(h\nu)^2=0$ and selecting the best linear component.

Figures (4) show the energy gap values of thin films (CdS) at different energies of the laser device, which shows the decrease in the energy gap with the increase in the energy of the source for all samples and this occurs due to the increase in the crystal size or due to the change of the lattice constant, also is because of the grain development, as well as a decrease in defect states near the bands, lowering the value of E_g [12], as there is an inverse relation between grain and E_g in nano size.

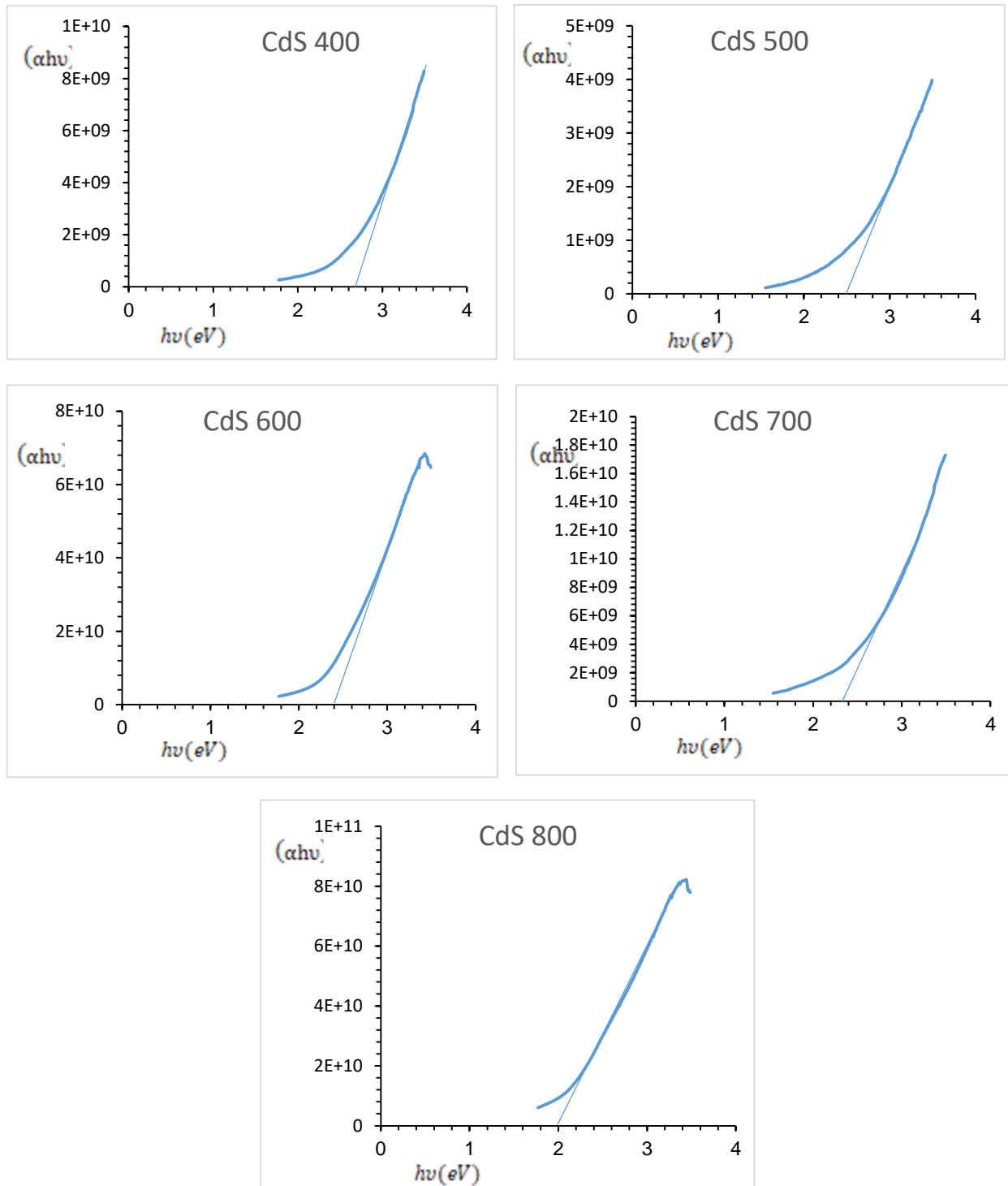


Figure (4): Tauc relation for CdS thin film prepared at different laser energies.

Conclusions

CdS films with a thickness of (200nm) were fabricated on glass substrates by laser induced plasma method. Films were prepared in vacuum at room temperature. Films were investigated by XRD, AFM, optical transmittance spectra and energy gap. Based on the above results, the following conclusions can be drawn;

1- The CdS films have a many peaks appeared to conform the lattice planes (100), (002), (101), (102), (110), (103). It is also evident that the peak's intensity increases while the peaks width is decreases with rising laser energy indicates on increasing the crystallinity and growing crystalline size

2- Increasing the laser pulses energy cause to increase in the average size and the surface roughness as shown.

3- Generally, with increasing laser energy, the transmittance of all deposited thin films decreases and also the energy gap decrease for all samples and this occurs due to the increase in the crystal size or due to the change of the lattice constant.

References

- S. K. Das and G. C. Morris, *J. Appl. Phys.*, 73, 782 (1993).
- Yoyo Hinuma, Fumiyasu Oba, Yoshitaro Nose, "First-principles study of valence band offsets at ZnSnP2/CdS, ZnSnP2/ZnS, and related chalcopyrite /zincblende heterointerfaces", *Journal of Applied Physics* 114, 043718, 31 July (2013).
- Maria Isabel Mendivil Palma, Bindu Krishnan, David Avellaneda Avellaneda, "Effect of wavelengths on the structure, morphology and optoelectronic properties of cadmium sulfide thin films by laser assisted chemical bath deposition Author links open overlay panel", *materialstoday PROCEEDINGS*, 25 September (2020).
- P. K. Nair, J. Campos, and M. T. S. Nair, *Semicond. Sci. Technol.*, 3, 134 (1988).
- M. Agata, H. Kurase, S. Hayashi and K. Yamamoto *Solid State Commun*, 76, 1061 (1990).
- C. T. Tsai, D. S. Chuu, G. L. Chen and S. L. Yang *J. Appl. Phys.*, 79, 9105 (1996).
- G. Perna, V. Capozzi, M. Ambrico, V. Augelli, T. Ligonzo, A. Minafra, L. Schiavulli and M. Pallara *Thin Solid Films* 453, 187 (2004).
- A. E. Abken, D. P. Halliday and K. Durose *J. Appl. Phys.* 105, 064515 (2009).
- C. S. Tepantlán, A. M. P. González and I. V. Arreola, *Revista Mexicana de Física*, 54, 2 112-117 (2008).
- [10] D. Bhattacharya "Plasma dynamics from laser ablated solid lithium" *Pramana J. Phys.*, vol. 55, N(5-6), (2000).
- J. Fred O'Shay "Time-Resolved Visible and Extreme Ultraviolet Spectroscopy of Laser-Produced Tin Plasma", Ph.D Dissertation, University of California, San Diego USA, (2007).
- V. K. Unnikrishnan, K. Alti, V. B. Kartha, C. Santhosh, G. P. Gupta, and B. M. Suri "Measurements of plasma temperature and electron density in laser-induced copper plasma by time-resolved spectroscopy of neutral atom and ion emissions", *Pramana - J. Phys.*, vol. 74, no. 6, pp. 983-993, (2010).